

Complex-Temperature Singularities in the $d = 2$ Ising Model: III. Honeycomb Lattice

Victor Matveev* and Robert Shrock**

Institute for Theoretical Physics
State University of New York
Stony Brook, N. Y. 11794-3840

Abstract

We study complex-temperature properties of the uniform and staggered susceptibilities χ and $\chi^{(a)}$ of the Ising model on the honeycomb lattice. From an analysis of low-temperature series expansions, we find evidence that χ and $\chi^{(a)}$ both have divergent singularities at the point $z = -1 \equiv z_\ell$ (where $z = e^{-2K}$), with exponents $\gamma'_\ell = \gamma'_{\ell,a} = 5/2$. The critical amplitudes at this singularity are calculated. Using exact results, we extract the behaviour of the magnetisation M and specific heat C at complex-temperature singularities. We find that, in addition to its zero at the physical critical point, M diverges at $z = -1$ with exponent $\beta_\ell = -1/4$, vanishes continuously at $z = \pm i$ with exponent $\beta_s = 3/8$, and vanishes discontinuously elsewhere along the boundary of the complex-temperature ferromagnetic phase. C diverges at $z = -1$ with exponent $\alpha'_\ell = 2$ and at $v = \pm i/\sqrt{3}$ (where $v = \tanh K$) with exponent $\alpha_e = 1$, and diverges logarithmically at $z = \pm i$. We find that the exponent relation $\alpha' + 2\beta + \gamma' = 2$ is violated at $z = -1$; the right-hand side is 4 rather than 2. The connections of these results with complex-temperature properties of the Ising model on the triangular lattice are discussed.

*email: vmatveev@max.physics.sunysb.edu

**email: shrock@max.physics.sunysb.edu

1 Introduction

There are several reasons for studying the properties of statistical mechanical models with the temperature variable generalised to take on complex values. First, one can understand more deeply the behaviour of various thermodynamic quantities by seeing how they behave as analytic functions of complex temperature. Second, one can see how the physical phases of a given model generalise to regions in appropriate complex-temperature variables. Third, a knowledge of the complex-temperature singularities of quantities which have not been calculated exactly helps in the search for exact, closed-form expressions for these quantities. This applies, in particular, to the susceptibility of the 2D Ising model, which has, to this day, never been calculated, in contrast to the (zero-field) free energy, first calculated (for the square lattice) by Onsager [1], and the spontaneous magnetisation, the expression for which (for the square lattice) was proposed by Onsager and first calculated by Yang [2]. A fourth reason for the interest in complex-temperature singularities is that they can significantly influence the behaviour of a given quantity for physical values of the temperature. Indeed, early studies [3, 4, 5] of such complex-temperature singularities were motivated in part by the fact that when they occurred closer to the origin, in a certain low-temperature expansion variable, than the physical critical point, they precluded the application of the ratio test, then in common use, to determine the location of this critical point. The first work on natural boundaries of the free energy of the Ising model (on the square lattice) for complex temperature was in Ref. [6].

Several years ago, we reported some results on complex-temperature singularities of the susceptibility and correlation length for the Ising model [7], including a discussion of complex-temperature symmetries and a proof (for the square lattice) that the (zero-field) susceptibility can have at most finite non-analyticities on the border of the complex-temperature extension of the symmetric phase, apart from its divergence at the physical critical point. Two recent papers have reported results on complex-temperature singularities for the Ising model on the square lattice [8, 9]. In Ref. [10], the present authors extended the study by Guttmann [5] of complex-temperature properties of the Ising model on the triangular lattice. In the present paper we shall carry out a study of the complex-temperature properties of the Ising model on the honeycomb (= hexagonal) lattice. For completeness we note that an analysis of complex-temperature singularities in the 3D Ising model, after those of Refs. [3, 4], was given in Ref. [11].

2 Complex-Temperature Extensions of Physical Phases

Our notation follows that in our previous papers [9, 10], so we review it here only briefly. We consider the Ising model on the honeycomb lattice (coordination number $q = 3$) at a temperature T and external magnetic field H defined by the partition function $Z = \sum_{\{\sigma_i\}} e^{-\beta\mathcal{H}}$ with the Hamiltonian

$$\mathcal{H} = -J \sum_{\langle ij \rangle} \sigma_i \sigma_j - H \sum_i \sigma_i \quad (2.1)$$

where $\sigma_i = \pm 1$ are the Z_2 spin variables on each site i of the lattice $\beta = (k_B T)^{-1}$, and J is the exchange constant. We use the standard notation $K = \beta J$, $h = \beta H$, $v = \tanh K$, $z = e^{-2K} = (1 - v)/(1 + v)$, and $u = z^2$. Another relevant variable is the elliptic modulus which one encounters in the broken-symmetry phases,

$$k_{<} = \frac{4z^{3/2}(1 - z + z^2)^{1/2}}{(1 - z)^3(1 + z)} \quad (2.2)$$

and its inverse, which occurs in expressions in the Z_2 -symmetric phase,

$$k_{>} = k_{<}^{-1} = \frac{4v^3}{(1 - v^2)^{3/2}(1 + 3v^2)^{1/2}} \quad (2.3)$$

We note the symmetries

$$K \rightarrow -K \Rightarrow \{v \rightarrow -v, \quad z \rightarrow 1/z, \quad u \rightarrow 1/u, \quad k_x \rightarrow -k_x\} \quad (2.4)$$

where $k_x = k_{<} \text{ or } k_{>}$. The reduced free energy per site is $f = -\beta F = \lim_{N_s \rightarrow \infty} N_s^{-1} \ln Z$ in the thermodynamic limit, where N_s is the number of sites on the lattice. The zero-field susceptibility is $\chi = \frac{\partial M(H)}{\partial H}|_{H=0}$, where $M(H)$ denotes the magnetisation. The staggered susceptibility is denoted $\chi^{(a)}$. It is convenient to deal with the reduced quantities $\bar{\chi} = \beta^{-1} \chi$ and $\bar{\chi}^{(a)} = \beta^{-1} \chi^{(a)}$. We recall that on a loose-packed lattice such as the honeycomb lattice, in the symmetric, paramagnetic (PM) phase, the uniform and staggered susceptibilities are simply related according to

$$\bar{\chi}^{(a)}(v) = \bar{\chi}(-v) \quad (2.5)$$

Following Onsager's solution for $f(K, h = 0)$ on the square lattice, the free energy was calculated for the honeycomb lattice in the papers of Ref. [12]. The spontaneous magnetisation for the honeycomb lattice was first given by Naya [13]. The critical coupling separating the symmetric, paramagnetic (PM) high-temperature phase from the phase with spontaneously broken Z_2 symmetry and ferromagnetic (FM) long-range order is $K_c = (1/4) \ln 3$, so that

$v_c = 1/\sqrt{3} = 0.577350\dots$ and $z_c = 2 - \sqrt{3} = 0.267949\dots$. As usual for loose-packed lattices, the critical point separating the PM phase from the phase with antiferromagnetic (AFM) long-range order is $K = -K_c$, or equivalently, $v = -v_c$, $z = 1/z_c = 2 + \sqrt{3}$.

We begin by discussing the phase boundaries of the model as a function of complex temperature, i.e. the locus of points across which the free energy is non-analytic. As noted in Ref. [7], there is an infinite periodicity in complex K under certain shifts along the imaginary K axis as a consequence of the fact that the spin-spin interaction $\sigma_i\sigma_j$ in \mathcal{H} is an integer. In particular, there is an infinite repetition of phases as functions of complex K ; these repeated phases are reduced to a single set by using the variables v or z owing to the symmetry relation $K \rightarrow K + ni\pi \Rightarrow \{v \rightarrow v, z \rightarrow z\}$. The requisite complex extensions of the physical phases can be seen by using the exact expression for the free energy [12],

$$f = \ln 2 + \frac{1}{4} \int_{-\pi}^{\pi} \int_{-\pi}^{\pi} \frac{d\theta_1 d\theta_2}{(2\pi)^2} \ln \left\{ \frac{1}{2} [\cosh^3(2K) + 1 - \sinh^2(2K)P(\theta_1, \theta_2)] \right\} \quad (2.6)$$

where

$$P(\theta_1, \theta_2) = \cos \theta_1 + \cos \theta_2 + \cos(\theta_1 + \theta_2) \quad (2.7)$$

The boundaries of the complex-temperature phases are comprised of the locus of points where the argument of the logarithm in f vanishes.¹ Expressed in terms of the low-temperature variable z , f is given by

$$f = \frac{q}{2}K + \frac{1}{4} \int_{-\pi}^{\pi} \int_{-\pi}^{\pi} \frac{d\theta_1 d\theta_2}{(2\pi)^2} \ln \left[(1+z)^2 \left\{ (1-2z+6z^2-2z^3+z^4) - 2z(1-z)^2 P(\theta_1, \theta_2) \right\} \right] \quad (2.8)$$

(where $q = 3$). Evidently, the argument of the logarithm vanishes along the curve defined by the solutions to the equation

$$(1 - 2z + 6z^2 - 2z^3 + z^4) - 2z(1 - z)^2 x = 0 \quad , \quad -\frac{3}{2} \leq x \leq 3 \quad (2.9)$$

where $x = P(\theta_1, \theta_2)$. This curve is shown in Fig. 1(a). (Note that the curve contains the point $z = -1$ where the initial factor $(1+z)^2$ vanishes.) Since eq. (2.9) has real coefficients, the solutions are either real or consist of complex conjugate pairs, which explains the reflection symmetry of the curve in Fig. 1(a) about the real axis in the z plane. Furthermore, under the transformation $z \rightarrow 1/z$, the left-hand side of eq. (2.9) retains its form, up to an overall factor of z^{-6} ; consequently the locus of solutions given by the curve in Fig. 1(a) is invariant under this mapping, $z \rightarrow 1/z$. For $x = 3$, eq. (2.9) has double roots at $z = z_c, 1/z_c$. As x decreases from 3 to -1 , the pairs of complex solutions move along the curve, rejoining again

¹ The free energy is trivially infinite at $K = \infty$; since this is an isolated point and hence does not form part of a boundary separating phases, it will not be important here.

in two pairs of double roots at $z = \pm i$ for $x = -1$. Finally, as x decreases from -1 to $-3/2$, the solutions move outward from $z = \pm i$ along the unit circle; the leftward-moving roots join at $z = -1$ while the rightward-moving roots terminate at the endpoints $z = e^{\pm i\pi/3}$. We shall denote the leftmost (ℓ) of the real roots as $z_\ell = -1$. The points $z = \pm i$ are singular points of the curve in the technical terminology of algebraic geometry [14]; specifically, they are multiple points of index 2, where two arcs of the curve cross each other (with an angle of $\pi/2$). We denote these as $z_{s\pm}$, respectively. The endpoints at $z = e^{\pm i\pi/3}$ are, of course, also singular points of the curve in the mathematical sense. The physical phases are: (i) FM, for $0 \leq z \leq z_c$; (ii) PM, for $z_c < z \leq 1$; and (iii) AFM, for $1 < z \leq \infty$. The complex-temperature extensions of these are the regions marked in Fig. 1(a). Note that the complex-temperature phase boundaries in Fig. 1(a) are formally the same as those for the Ising model on the triangular lattice, in the v plane (shown in Fig. 1(c) in Ref. [10]). This is a consequence of the geometric duality of the honeycomb and triangular lattices. Recall, however, that the actual phase structures, both for physical and complex temperature, are different; in particular, the model on the triangular lattice has no AFM phase, and the outer phase in the v plane (denoted O in Ref. [10]) has no overlap with any physical phase.

The transformation from z to the elliptic modulus $k_<$ given in eq. (2.2) maps the z plane to the image shown in Fig. 1(b). As noted in (2.4), z and $1/z$ are mapped to $k_<$ and $-k_<$, respectively. The point z_c is mapped to $k_< = 1$. The three points $1/z_c$ and $\pm i$ are all mapped to $k_< = -1$. The point $z = 0$, as well as the points at complex infinity (i.e., $z = \lim_{\rho \rightarrow \infty} \rho e^{i\theta}$ for arbitrary real θ) are mapped to $k_< = 0$. In addition, given the factorisation $(1 - z + z^2) = (z - e^{i\pi/3})(z - e^{-i\pi/3})$, it follows that the finite endpoints $z = e^{\pm i\pi/3}$ are mapped to $k_< = 0$. This latter property has the consequence that this elliptic modulus variable is not a useful one in which to re-express the low-temperature series expansion for $\bar{\chi}$, in contrast to the case of the square lattice, where the analogous variable $k_<$ played a very valuable role. The transformation given by (2.2) maps the complex-temperature FM and AFM phases formally onto the same phase, occupying the interior of the unit circle in the $k_<$ plane; similarly, it maps the complex-temperature PM phase onto the exterior of this circle. The complex conjugate arcs of the unit circle from $\arg(z) = \pm\pi/3$ to $\arg(z) = \pm\pi/2$ are mapped onto the same line segment extending along the negative real axis in the ($k_<$) plane from 0 to -1 , while the complex conjugate arcs of the unit circle from $\arg(z) = \pm\pi/2$ to $z = -1$ are mapped onto the negative real axis from $k_< = -1$ to $k_< = -\infty$. As usual with a singular point, the image of the point $z = -1$ depends on the direction in which one approaches it in the z plane; for example, if one approaches this point along the negative real z axis (with a infinitesimal positive imaginary part so that with the branch cut for the $z^{3/2}$ factor being placed along the negative real axis, $(-1)^{3/2}$ evaluates to $-i$), the image

approaches $k_< = -i\infty$, and so forth for other directions.

One may work out the phase boundaries for the honeycomb lattice in the v plane either by transforming the boundaries in the z plane using the bilinear conformal mapping $v = (1 - z)/(1 + z)$, or directly by analysing the free energy expressed in terms of v , viz.,

$$f = \ln 2 - \frac{3}{4} \ln(1 - v^2) + \frac{1}{4} \int_{-\pi}^{\pi} \int_{-\pi}^{\pi} \frac{d\theta_1 d\theta_2}{(2\pi)^2} \ln[1 + 3v^4 - 2v^2(1 - v^2)P(\theta_1, \theta_2)] \quad (2.10)$$

(The second term is just the usual $(q/2) \ln(\cosh K)$ term.) Aside from the trivial infinity at $v = 1$ ($K = \infty$), the locus of singularities of f is given by the solutions to the equation $1 + 3v^4 - 2v^2(1 - v^2)x = 0$ for $-3/2 \leq x \leq 3$. This is shown in Fig. 1(c). This equation has real coefficients and is invariant under the transformation $v \rightarrow -v$; the respective consequences of these two properties are that the solution curve in Fig. 1(c) is invariant under reflection about the horizontal and vertical axes in the v plane. The vertical line segments extend from $\pm i/\sqrt{3}$ to $\pm i\infty$, respectively, and are the images, under the conformal mapping, of the portion of boundary in the z plane lying on the unit circle. The curve in Fig. 1(c) is formally the same as the complex-temperature phase boundary for the Ising model on the triangular lattice in the variable z , because of the duality noted above.

Using the general fact that the high-temperature and (for discrete spin models such as the Ising model) the low-temperature expansions have finite radii of convergence, we can use standard analytic continuation arguments to establish that in addition to the free energy and its derivatives, also the magnetisation and susceptibility are analytic functions within each of the complex-temperature phases. This defines these functions as analytic functions of the respective complex variable (K , v , or z , etc.). Of course, these functions are, in general, complex away from the physical line $-\infty < K < \infty$.

Our definition of singular forms of a function at a complex-temperature singular point was given in Ref. [9, 10]. Note, in particular, that whereas a physical critical point can only be approached from two different phases, high- or low-temperature, some complex-temperature singular points may be approached from more than two phases.

The low-temperature series for the staggered susceptibility is expressed in terms of the variable $y = 1/z$, and for our analysis of this series, we observe that the complex-temperature phase diagram in the y plane has the same phase boundaries as those in Fig. 1(a), owing to the invariance of this boundary under $z \rightarrow 1/z$. The phases are, of course, inverted, so that the innermost phase is AFM, to its right, PM, and, in the outer region, FM.

Finally, because of the star-triangle relations connecting the Ising model on the triangular and honeycomb lattices, the following exact relations hold [20]:

$$\chi_t(u) = \frac{1}{2} [\chi_{hc}(z') + \chi_{hc}^{(a)}(z')] \quad (2.11)$$

where

$$u = \frac{z'}{1 - z' + z'^2} \quad (2.12)$$

and

$$\chi_t(w) = \frac{1}{2} [\chi_{hc}(v) + \chi_{hc}^{(a)}(v)] = \frac{1}{2} [\chi_{hc}(v) + \chi_{hc}(-v)] \quad (2.13)$$

where

$$v^2 = \frac{w}{1 - w + w^2} \quad (2.14)$$

3 Complex-Temperature Behaviour of the Specific Heat

3.1 General

From the exact expression (2.8) for the free energy f we calculate the specific heat in the low-temperature phase as

$$k_B^{-1} K^{-2} C = -\frac{8z^2}{(1-z^2)^2} + \frac{[3 - 12(z+z^7) + 28(z^2+z^6) - 20(z^3+z^5) + 18z^4]}{\pi(1+z)(1-z)^5(1-z+z^2)} K(k_<) - \frac{3(1-z)(1+z)}{\pi(1-z+z^2)} E(k_<) \quad (3.1.1)$$

where $K(k) = \int_0^{\pi/2} d\theta [1 - k^2 \sin^2 \theta]^{-1/2}$ and $E(k) = \int_0^{\pi/2} d\theta [1 - k^2 \sin^2 \theta]^{1/2}$ are the complete elliptic integrals of the first and second kinds, respectively, which depend on the (square of the) elliptic modulus k , and $k_<$ was given in eq. (2.2).² The expression (3.1.1) applies in both the physical FM and AFM phases, and may be analytically continued throughout the respective complex-temperature extensions of these phases.

In the physical PM phase, a similar calculation starting from (2.6) or (2.10) yields

$$k_B^{-1} K^{-2} C = v^{-2} (1-v^2)^{1/2} \left[-\frac{1}{2} (1-v^2)^{3/2} + \frac{4}{\pi(1+3v^2)^{1/2}} K(k_>) - \frac{3(1-v^2)}{\pi(1+3v^2)^{1/2}} E(k_>) \right] \quad (3.1.2)$$

where $v = \tanh K$, and $k_>$ was given in (2.3). Having these exact expressions for the specific heat, we proceed to work out its behaviour at complex-temperature singularities.

²In passing, we note that Houtappel's expressions for the internal energy and specific heat, eqs. (108) and (109), respectively, in Ref. [12], are incorrect if one uses the integrals $\epsilon_1(\beta)$ and $\epsilon_2(\beta)$ as he defines them, with the range of integration from $\phi = 0$ to 2π . If, instead, one takes the range of integration from $\phi = 0$ to $\phi = \pi/2$, so that the integrals are just the usual elliptic integrals $K(\sqrt{\beta})$ and $E(\sqrt{\beta})$, then his eqs. (108) and (109) become correct.

3.2 Vicinity of $z = -1$

As one approaches the point $z = -1$ (denoted z_ℓ as above) from within either the complex-temperature FM or AFM phase, the specific heat diverges, with the dominant divergence arising from the first term in (3.1.1), which becomes $-2(1+z)^{-2}$. (There is also a weaker, logarithmic divergence from the term involving $K(k_<)$.) Hence, we find

$$\alpha'_{\ell,FM} = \alpha'_{\ell,AFM} = 2 \quad (3.2.1)$$

Now, $K = -(1/2) \ln z$, so choosing the branch cut for the complex logarithm to lie along the negative real axis and choosing the first Riemann sheet for the evaluation of the logarithm, as z approaches -1 from above or below the negative real axis, one has $K_\ell = \mp i\pi/2$ respectively, and hence in both cases

$$k_B^{-1}C \rightarrow \frac{\pi^2}{2(1+z)^2} \quad , \quad as \quad z \rightarrow -1 \quad (3.2.2)$$

It is interesting to relate the critical exponent (3.2.1) to the critical exponent α'_e for the specific heat on the triangular lattice at the point $u = u_e = -1/3$, which corresponds, via (2.12), to $z' = z = -1$ on the honeycomb lattice. (Recall that the point $u = -1/3$ is an endpoint of a singular line segment protruding into the complex-temperature FM phase; hence, it can only be approached from within this phase, and so $\alpha'_e \equiv \alpha'_{e,FM}$.) In Ref. [10], using the exact expression for the free energy on the triangular lattice, we calculated that $\alpha'_e = 1$. Given the star-triangle relations which connect the Ising model on these two lattices and the fact that the Taylor series expansion of $u + 1/3$, as a function of z' , in the vicinity of $z' = -1$ ($= z$ on the honeycomb lattice), starts with the quadratic term,

$$u + \frac{1}{3} = \frac{1}{9}(1+z')^2 + \frac{1}{9}(1+z')^3 + O((1+z')^4) \quad (3.2.3)$$

it follows that the exponents $\alpha'_{\ell,FM} = \alpha'_{\ell,AFM} = 2$ at $z = -1$ on the honeycomb lattice have twice the value of $\alpha'_e = 1$ at $u = -1/3$ on the triangular lattice. Note, however, that the leading divergence in C arises from different terms on the two different lattices (in the triangular lattice, the leading divergence arises from the term proportional to $E(k_<)$, as discussed in Ref. [10]).

3.3 Vicinity of $z = \pm i$

The points $z = \pm i$ can be approached from within the complex-temperature extensions of the FM, AFM, and PM phases. For the approach to $z = \pm i$ from within the complex FM and AFM phases, we find from (3.1.1) that the first term and the term involving $E(k_<)$ yield finite

contributions, while the term involving $K(k_<)$ diverges logarithmically, as $\pm(4i/\pi)K(k_< \rightarrow -1)$. Using the fact that as $\lambda \rightarrow \pm 1$, $K(\lambda) \rightarrow (1/2)\ln(16/(1-\lambda^2))$, and the Taylor series expansion of $k_<^2$ in the neighborhood of $z = \pm i$,

$$k_<^2 = 1 - 2(z \mp i)^3 + O((z \mp i)^4) \quad (3.3.1)$$

we can express the most singular term on the RHS of eq. (3.1.1) as $\mp(2i/\pi)\ln[(z \mp i)^3]$. Evaluating $K = -(1/2)\ln z$ for $z = \pm i$ on the first Riemann sheet of the logarithm, we have $K = \mp i\pi/4$, so that

$$k_B^{-1}C \sim \pm \frac{i}{8\pi} \ln[(z \mp i)^3] \quad (3.3.2)$$

It follows that for $z = z_{s,\pm} = \pm i$,

$$\alpha'_{s,FM} = \alpha'_{s,AFM} = 0 \quad (\log. \text{ div.}) \quad (3.3.3)$$

These results are the same as we found for the specific heat exponent on the triangular lattice at the point $u = -1$ corresponding, via (2.12) with $z' \equiv z$, to $z = \pm i$ on the honeycomb lattice.

For the approach to the points $v = v_{s\pm} = \pm i$ from within the complex-temperature PM phase, we use the expression for C in this phase, eq. (3.1.2). We find that the term involving $K(k_>)$ produces a logarithmically divergence in C , so that the specific heat exponent $\alpha_{s,PM} \equiv \alpha_s$ is

$$\alpha_s = 0 \quad (\log. \text{ div.}) \quad (3.3.4)$$

Taking the branch cuts for the factor $(1+3v^2)^{1/2}$ to lie along the semi-infinite line segments from $\pm i/\sqrt{3}$ to $\pm i\infty$, and taking the approach such that $(-1)^{1/2}$ is evaluated as $+i$, we find that this term yields $(2i/\pi)\ln[(1-k_>^2)]$. Using the Taylor series expansion of $k_>^2$, as a function of v , near $v = i$,

$$k_>^2 = 1 - 2i(v - i)^3 + O((v - i)^4) \quad (3.3.5)$$

and its complex conjugate for $v \rightarrow -i$, and the result $K = \operatorname{arctanh}(\pm i) = \pm i\pi/4$, we find

$$k_B^{-1}C \sim -\frac{i\pi}{8} \ln[(v \mp i)^3] \quad (3.3.6)$$

(In the evaluation of the function $\operatorname{arctanh}(\zeta) = (1/2)\ln[(1+\zeta)/(1-\zeta)]$ here and below, we again use the first Riemann sheet of the logarithm.)

3.4 Vicinity of $v = \pm i(3)^{-1/2}$

We next determine the singularities of the specific heat as one approaches the endpoints $v = \pm v_e = \pm i/\sqrt{3}$ of the semi-infinite line segments protruding into the complex-temperature PM phase. Note that all directions of approach to $v = \pm i/\sqrt{3}$ except exactly (down or up, respectively) along the singular line segments occur from within the complex PM phase. From (3.1.2) we find that C is divergent, with the leading divergence arising from the term involving $E(k_>)$. This term gives $\pm(4\sqrt{3}/\pi)(1 + 3v^2)^{-1}$ as $v \rightarrow \pm i$, so

$$\alpha_e = 1 \tag{3.4.1}$$

Using $K = \operatorname{arctanh}(\pm i/\sqrt{3}) = \pm i\pi/6$, we have

$$k_B^{-1}C \rightarrow \mp \frac{\pi}{3^{3/2}(1 + 3v^2)} \quad \text{as } v \rightarrow \pm \frac{i}{\sqrt{3}} \tag{3.4.2}$$

3.5 Elsewhere on the Complex-Temperature Phase Boundary

The free energy $f(K)$ is non-analytic across the complex-temperature phase boundaries, and hence, of course, this is also true of its derivatives with respect to K , in particular the internal energy U and the specific heat C . As an illustration, consider moving along a ray outward from the origin of the z plane defined by $z = re^{i\theta}$ with $\theta < \pi/2$. For a given θ , as r exceeds the critical value $r_c(\theta)$, one passes from the complex-temperature FM phase into the complex-temperature PM phase. At the phase boundary, as is clear from Fig. 1(b), the elliptic modulus $k_<$ has magnitude unity and can be written $k_< = e^{i\phi}$, where the angle ϕ depends on θ . As we discussed in connection with Fig. 1(b), $z = z_c$ is mapped to $k_< = 1$, and $z = i$ to $k_< = -1$; ϕ increases from 0 at $\theta = 0$ to π at $\theta = \pi/2$. Hence, for $0 < \theta < \pi/2$, $k_<$ has a nonzero imaginary part. Now when one passes through the FM-PM phase boundary along the ray at this angle θ , one changes the argument of the elliptic integrals from $k_< = e^{i\phi}$ to $k_> = 1/k_< = e^{-i\phi}$. The elliptic integrals $K(k)$ and $E(k)$ are analytic functions of k^2 with, respectively, a logarithmically divergent and a finite branch point singularity at $k^2 = 1$ and associated branch cuts which may be taken to lie along the positive real axis in the k^2 plane. In particular, $K(k)$ and $E(k)$ are both analytic at the point $k = k_< = e^{i\phi}$ for $0 < \theta < \pi/2$. Hence, when we replace the argument $k_<$ by $k_>$, which is the complex conjugate of $k_<$ on the unit circle, we have $F(k_> = e^{-i\phi}) = F(k_< = e^{i\phi})^*$ for $F = K, E$. Since these elliptic integrals are complex for generic complex $k_<$, it follows that their imaginary part is discontinuous across the FM-PM boundary. The coefficients of the elliptic integrals are also different functions in the FM and PM phases, and these coefficients are discontinuous as one crosses the boundary between these phases on the above ray. Combining these, we find that

the specific heat itself is discontinuous as one moves across the FM-PM boundary on this ray.

4 Complex-Temperature Behaviour of the Spontaneous Magnetisation

The spontaneous magnetisation is given in the physical FM phase by [13]

$$\begin{aligned} M_{hc} &= (1 - (k_<)^2)^{1/8} \\ &= \frac{(1 + z^2)^{3/8}(1 - 4z + z^2)^{1/8}}{(1 - z)^{3/4}(1 + z)^{1/4}} \end{aligned} \quad (4.1)$$

and vanishes identically elsewhere. Observe that $(1 - 4z + z^2) = (1 - z/z_c)(1 - z_c z)$. The expression (4.1) for M can be analytically continued throughout the complex-temperature extension of the physical FM phase. It evidently vanishes continuously at both the physical critical point $z = z_c$, with critical exponent $\beta = 1/8$, and at the complex-temperature points $z = z_{s\pm} = \pm i$, with exponent

$$\beta_s = \frac{3}{8} \quad (4.2)$$

As we have observed earlier [9], this exponent is the same as the exponent $\beta_{s,t} = 3/8$ characterising the zero in the magnetisation on the triangular lattice at the point $u = -1$ corresponding, via eq. (2.12), to $z' = z = \pm i$ on the honeycomb lattice; however, $\beta_{s,hc} = \beta_{s,t}$ differ from $\beta_{s,sq} = 1/4$ characterising the zero in M on the square lattice at $u = -1$. This is a violation of universality, since this critical exponent is evidently lattice-dependent. A way of understanding the origin of this violation was discussed in Ref. [9] and directly reflects the fact that the Hamiltonian and hence the internal energy are not, in general, real numbers at complex-temperature singular points.

Furthermore, M has a divergence at $z = z_\ell = -1$, with exponent

$$\beta_\ell = -\frac{1}{4} \quad (4.3)$$

Note that the apparent zero at $z = 1/z_c$ and the apparent divergence at $z = 1$ do not actually occur, since these points are outside of the complex-temperature extensions of the FM phase, in which the (analytic continuation of the) formula (4.1) applies. We recall that, as a consequence of the star-triangle relation which connects the Ising model on the triangular and honeycomb lattices [21],

$$M_t(u) = M_{hc}(z') \quad (4.4)$$

u, t	z, hc	M	β, t	β, hc
$u_c = 1/3$	$z_c = 2 - \sqrt{3}$	0 (cont.)	1/8	1/8
-1	$\pm i$	0 (cont.)	3/8	3/8
-1/3	-1	div.	-1/8	-1/4

Table 1: Comparative singularities of M on the triangular (t) and honeycomb (hc) lattices. Points are related according to the transformation (2.12) with $z' = z$ (hc). The notations 0 (cont.) and div. denote, respectively, a point where M vanishes continuously and where it diverges.

where [22]

$$M_t = \left(\frac{1+u}{1-u}\right)^{3/8} \left(\frac{1-3u}{1+3u}\right)^{1/8} \quad (4.5)$$

and z' ($= z$ on the honeycomb lattice) was given in eq. (2.12).

In Table 2 we list a comparison of singularities in M_t and M_{hc} . Note that, aside from the points listed in this table, these functions vanish discontinuously along the borders of the respective complex-temperature FM phases. The fact that the exponent β_ℓ with which M_{hc} diverges at the point $z = -1$ on the honeycomb lattice is twice the exponent with which M_t diverges at the point $u = -1/3$ on the triangular lattice (which corresponds to $z' = z = -1$ via (2.12)) follows from the star-triangle relation connecting the Ising model on these two lattices and the property that the Taylor series expansion of $u + 1/3$, as a function of z' , in the vicinity of $z' = -1$, starts with the quadratic term, as given in eq. (3.2.3).

Since the honeycomb lattice is loose-packed, one immediately infers the staggered magnetisation $M_{hc,st}$ from the (uniform) magnetisation M_{hc} : formally,

$$M_{hc,st}(y) = M_{hc}(z \rightarrow y) \quad (4.6)$$

Hence, $M_{hc,st}$ has continuous zeros at both the physical critical point $y = y_c$ and the complex-temperature point $y = -1$, and diverges at the points $y = \pm i$.

5 Analysis of the Low-Temperature Series for $\bar{\chi}$

5.1 General

Here we shall study the complex-temperature singularities of the susceptibility $\bar{\chi}$ which occur as one approaches the boundary of the (complex-temperature extension of the) FM phase

from within this phase. In the next section we shall carry out a similar analysis for the staggered susceptibility, $\bar{\chi}^{(a)}$. In particular, we consider the behaviour in the vicinity of the points $z = -1$ and $z = \pm i$. For the study of $\bar{\chi}$, we use the low-temperature series expansion for $\bar{\chi}$, which is given by

$$\bar{\chi} = 4z^3 \left(1 + \sum_{n=1}^{\infty} c_n z^n \right) \quad (5.1.1)$$

For the study of $\bar{\chi}^{(a)}$, we use the corresponding low-temperature series expansion

$$\bar{\chi}^{(a)} = 4y^3 \left(1 + \sum_{n=1}^{\infty} c_{n,a} y^n \right) \quad (5.1.2)$$

where $y = 1/z$ is the expansion variable in the AFM phase. These expansions have finite radii of convergence and, by analytic continuation from the physical low-temperature intervals $0 \leq z < z_c$ and $0 \leq y \leq y_c$, apply throughout the complex-temperature extensions of the FM and AFM phases, respectively. (Here y_c is the critical point separating the PM and AFM phases. As can be seen from Fig. 1(a), this occurs at $z = 1/z_c = 2 + \sqrt{3}$, so that $y_c = 2 - \sqrt{3}$, the same numerical value as the critical point z_c separating the PM and FM phases.) Since the z^3 and y^3 factors are known exactly in the respective series expansions (5.1.1) and (5.1.2), it is convenient to study the remaining factors $\bar{\chi}_r = \bar{\chi}/(4z^3)$ and $\bar{\chi}_r^{(a)} = \bar{\chi}^{(a)}/(4y^3)$. For the honeycomb lattice, the expansion coefficients c_n and $c_{n,a}$ were calculated by the King's College group to order $n = 13$ (i.e., $\bar{\chi}$ and $\bar{\chi}^{(a)}$ to $O(z^{16})$) in 1971 [15], and to order $n = 18$ (i.e., $\bar{\chi}$ and $\bar{\chi}^{(a)}$ to $O(z^{21})$) in 1975 [16]. We have checked and found that apparently these series have not been calculated to higher order subsequently [17, 18]. We have analysed these series using dlog Padé and differential approximants (a recent review of the methods is given in Ref. [19]). For the approach to $z = -1$ (denoted z_ℓ) from within the complex-temperature extension of the FM phase, we write the leading singularity of $\bar{\chi}$ as

$$\bar{\chi}(z) \sim A'_\ell |1 - z/z_\ell|^{-\gamma'_\ell} (1 + a_{1,\ell} |1 - z/z_\ell| + \dots) \quad (5.1.3)$$

where A'_ℓ and γ'_ℓ denote, respectively, the critical amplitude and critical exponent, and the dots ... represent analytic confluent corrections. Similarly, for the approach to this point, which in this context we denote $y_\ell = 1/z_\ell = -1$, from within the complex-temperature extension of the AFM phase, we write the leading singularity of $\bar{\chi}^{(a)}$ as

$$\bar{\chi}^{(a)}(y) \sim A'_{\ell,a} |1 - y/y_\ell|^{-\gamma'_{\ell,a}} (1 + a_{1,\ell,a} |1 - y/y_\ell| + \dots) \quad (5.1.4)$$

(As is clear from Fig. 1(a), this point $z = 1/y = -1$ can only be approached from within the complex-temperature FM or AFM phases.) As in our earlier studies of complex-temperature singularities of $\bar{\chi}$ in the Ising model on the square and triangular lattices [9, 10], we have

not included non-analytic confluent corrections to the scaling form in eq. (5.1.3) since, as we have discussed before, previous work has indicated that they are very weak or absent for the usual critical point of the 2D Ising model.

Before proceeding, we consider the implications of the exact relation (2.11). Given that $\chi_t(u)$ has a singularity at $u = u_e = -1/3$, it follows that the sum $\chi_{hc}(z') + \chi_{hc}^{(a)}(z')$ on the honeycomb lattice has the same singularity at the point $z' = 1$ corresponding via (2.12) to $u = -1/3$. But this does not, by itself, determine the singularities in the individual functions χ_{hc} and $\chi_{hc}^{(a)}$ at this point. If one could prove that both χ_{hc} and $\chi_{hc}^{(a)}$ necessarily have the same singularity at $z' = -1$, then the relation (2.11), together with the result that $\chi_t(u) \sim (1 + 3u)^{-\gamma'_e}$ with $\gamma'_e = 5/4$ [5, 10], and the Taylor series expansion of $u + 1/3$ as a function of z' (i.e., z on the honeycomb lattice) in the vicinity of $z' = -1$, eq. (3.2.3), would imply that $\gamma'_\ell = \gamma'_{\ell,a} = 2\gamma'_e = 5/2$. However, although it is plausible that χ_{hc} and $\chi_{hc}^{(a)}$ do have the same singularities at $z = -1$, there is no simple relationship between the respective low-temperature series for these two functions, as is clear from the first few terms [15],

$$\bar{\chi} = 4z^3 [1 + 6z + 27z^2 + 122z^3 + 516z^4 + 2148z^5 + \dots] \quad (5.1.5)$$

and

$$\bar{\chi}^{(a)} = 4y^3 [1 + 0 \cdot y + 3y^2 + 2y^3 + 12y^4 + 24y^5 + \dots] \quad (5.1.6)$$

Hence, an explicit series analysis is worthwhile to obtain the critical exponents.

5.2 Exponent at $z = -1$ Singularity

Since, as expected, we obtained more precise results from the differential approximants than the dlog Padé approximants, we shall concentrate on the former here. Our notation follows that of Guttmann [19] and our earlier papers [9, 10], so we shall only describe it briefly. In this method, the function $f = \bar{\chi}_r(\zeta)$ being approximated satisfies a linear ordinary differential equation (ODE) of K' th order, $\mathcal{L}_{M,L} f_K(\zeta) = \sum_{j=0}^K Q_j(\zeta) D^j f_K(\zeta) = R(\zeta)$, where $Q_j(\zeta) = \sum_{\ell=0}^{M_j} Q_{j,\ell} \zeta^\ell$ and $R(\zeta) = \sum_{\ell=0}^L R_\ell \zeta^\ell$ (and ζ denotes a generic complex variable). We shall use the implementation of the method in which $D \equiv \zeta d/d\zeta$. The solution to this ODE, with the initial condition $f(0) = 1$, is the resultant approximant, labelled as $[L/M_0; \dots; M_K]$. The general solution of the ODE has the form $f_j(\zeta) \sim A_j(\zeta) |\zeta - \zeta_j|^{-p_j} + B(\zeta)$ for $\zeta \rightarrow \zeta_j$. The singular points ζ_j are determined as the zeroes of $Q_K(\zeta)$ and are regular singular points of the ODE, and the exponents are given by $-p_j = K - 1 - Q_{K-1}(\zeta_j)/(Q_j Q'_K(\zeta_j))$. We recall that if the series for the function is calculated to order ζ^N , then one can compute the differential approximants $[L/M_0; M_1]$ up to order $L + M_0 + M_1 = N - 2$. We shall list the results from the differential approximants from to $\bar{\chi}_r$ and $\bar{\chi}_r^{(a)}$ from $L + M_0 + M_1 = 13$ to the

$[L/M_0; M_1]$	z_{sing}	$ z_{sing} - z_\ell $	γ'_ℓ
[1/6; 6]	-1.0096461	9.6×10^{-3}	2.5188
[1/6; 7]	-1.0009020	9.0×10^{-5}	2.3989
[1/7; 5]	-1.0056732	5.7×10^{-3}	2.4418
[2/6; 6]	-1.0047536	4.8×10^{-3}	2.4588
[2/7; 5]	-0.9945961	5.4×10^{-3}	2.2967
[3/6; 7]	-0.9959243	4.1×10^{-3}	2.4136
[3/7; 6]	-0.9903576	9.6×10^{-3}	2.3022
[4/4; 6]	-0.9948731	5.1×10^{-3}	2.1301
[4/6; 6]	-0.9946423	5.4×10^{-3}	2.3580
[5/4; 5]	-1.0007133	7.1×10^{-5}	2.1252
[5/4; 6]	-1.0064564	6.5×10^{-3}	2.0704

Table 2: Values of z_{sing} and γ'_ℓ from differential approximants to low-temperature series for $\bar{\chi}_r(z)$. See text for definition of $[L/M_0, M_1]$ approximant. We only display entries which satisfy the accuracy criterion $|z_{sing} - z_\ell| \leq 10^{-2}$, where $z_\ell = -1$.

maximum value possible using the series for these functions calculated to $O(z^{18})$ and $O(y^{18})$, viz., $L + M_0 + M_1 = 16$. We take $K = 1$, which will be adequate for our purposes, and use unbiased differential approximants since this allows us to apply an extrapolation technique as in our earlier work. In this technique, we plot the value of the exponent obtained from each differential approximant as a function of the distance of the corresponding pole location from the inferred exact position of the singularity (e.g., $z = -1$, etc.). We then extrapolate to zero distance of the pole from this singularity to obtain the estimate of the exponent. Of course, this is essentially equivalent to using biased differential approximants. We present our results in Table 2.

These results yield evidence that $\bar{\chi}$ has a divergent singularity at $z = -1$, as one approaches this point from the complex-temperature FM phase. Since the values of the exponent from the differential approximants show considerable scatter, it is only possible to extract a rather crude estimate for γ'_ℓ . We obtain

$$\gamma'_\ell = 2.4 \pm 0.2 \tag{5.2.1}$$

This is consistent with the following inference which we shall make for the exact value of this exponent:

$$\gamma'_\ell = \frac{5}{2} \tag{5.2.2}$$

We note that the low-temperature series does not yield as precise a determination of this exponent at $z = -1$ on the honeycomb lattice as the corresponding low-temperature series did for the susceptibility exponent on the triangular lattice at the point $u = -1/3$ related to $z = z' = -1$ via (2.12) [5, 10]. The critical amplitude A'_ℓ for the susceptibility at $z = -1$ will be discussed below.

6 Analysis of the Low-Temperature Series for $\bar{\chi}^{(a)}$

6.1 General

The staggered susceptibility $\bar{\chi}^{(a)}$ has a well-known divergent singularity at $y = y_c = 2$ with low-temperature exponent $\gamma^{(a)'} = 7/4$. Here we analyse the complex-temperature singularities of this function using the low-temperature series given above in eq. (5.1.2).

6.2 Critical Exponent of $\bar{\chi}^{(a)}$ at $z = -1$ Singularity

Our results from the differential approximants are listed in Table 3. From these we find strong evidence that as one approaches the point $y = 1/z = -1$ from within the complex AFM phase, $\bar{\chi}^{(a)}$ has a divergent singularity. It is interesting that the exponent values from these differential approximants show less scatter than those which we found for the uniform susceptibility. Furthermore, there is a better correlation between the value of the exponent and the distance of the pole location from the inferred exact value of the singularity in Table 3, as compared with Table 2. Using our extrapolation technique, we obtain

$$\gamma'_{\ell,a} = 2.50 \pm 0.02 \quad (6.2.1)$$

This is consistent with the following exact value, which we infer:

$$\gamma'_{\ell,a} = \frac{5}{2} \quad (6.2.2)$$

so that, with this inference,

$$\gamma'_{\ell,a} = \gamma'_\ell \quad (6.2.3)$$

6.3 Comment on Exponent Relations at $z = -1$

Using the exact results $\alpha'_{\ell,FM} = 2$ from eq. (3.2.1) and $\beta_\ell = -1/4$ from eq. (4.3), and our conclusion from series analysis that $\gamma'_{\ell,FM} = 5/2$, we find that

$$\alpha'_{\ell,FM} + 2\beta_\ell + \gamma'_{\ell,FM} = 4 \quad (6.3.1)$$

$[L/M_0; M_1]$	y_{sing}	$ y_{sing} - y'_\ell $	$\gamma'_{\ell,a}$
[0/7; 6]	-0.9987578	1.2×10^{-3}	2.4468
[0/7; 7]	-0.9901632	9.8×10^{-3}	2.3222
[0/7; 8]	-0.9993457	6.5×10^{-4}	2.4810
[0/7; 9]	-1.0035955	3.6×10^{-3}	2.5718
[0/8; 7]	-0.9951663	4.8×10^{-3}	2.3996
[0/9; 7]	-1.0015320	1.5×10^{-3}	2.5192
[1/6; 7]	-0.9952671	4.7×10^{-3}	2.4076
[1/6; 8]	-1.0013204	1.3×10^{-3}	2.5237
[1/7; 6]	-0.9924817	7.5×10^{-3}	2.3586
[1/8; 6]	-0.9987880	1.2×10^{-3}	2.4668
[2/5; 7]	-0.9925676	7.4×10^{-3}	2.3391
[2/6; 6]	-0.9958472	4.2×10^{-3}	2.4235
[2/6; 7]	-0.9958755	4.1×10^{-3}	2.4243
[2/6; 8]	-1.0031308	3.1×10^{-3}	2.5572
[2/7; 5]	-1.0018189	1.8×10^{-3}	2.5643
[2/7; 6]	-0.9959874	4.0×10^{-3}	2.4265
[2/8; 6]	-1.0000820	8.2×10^{-5}	2.4837
[3/6; 4]	-1.0099574	1.0×10^{-2}	2.7256
[3/6; 5]	-1.0042365	4.2×10^{-3}	2.6064
[3/6; 6]	-0.9960860	3.9×10^{-3}	2.4283
[3/6; 7]	-1.0029001	2.9×10^{-3}	2.5645
[3/7; 6]	-0.9998642	1.4×10^{-4}	2.4976
[4/6; 4]	-1.0036469	3.6×10^{-3}	2.6153
[4/6; 5]	-1.0083269	8.3×10^{-3}	2.5168
[4/6; 6]	-0.9983598	1.6×10^{-3}	2.4518
[5/4; 6]	-1.0096131	9.6×10^{-3}	2.4347
[5/5; 6]	-1.0004620	4.6×10^{-4}	2.4251
[5/6; 4]	-0.9932140	6.8×10^{-3}	2.4105
[5/6; 5]	-0.9975739	2.4×10^{-3}	2.4589

Table 3: Values of y_{sing} and $\gamma'_{\ell,a}$ from differential approximants to low-temperature series for $\bar{\chi}_r^{(a)}(y)$. See text for definition of $[L/M_0, M_1]$ approximant. We only display entries which satisfy the accuracy criterion $|y_{sing} - y_\ell| \leq 10^{-2}$, where $y_\ell = -1$.

The right-hand side of eq. (6.3.1) is twice the value at physical critical points. We have given an explanation above of why the exponents $\alpha'_{\ell,FM}$ and β_ℓ for the singularity at $z = -1$ on the honeycomb lattice have twice the values of the respective exponents on the triangular lattice, at the point $u = -1/3$ which corresponds, via eq. (2.12) to $z' = z = -1$ on the honeycomb lattice; this followed from the star-triangle relation connecting the Ising model on these two lattices together with the fact that the Taylor series expansion of $u + 1/3$, as a function of z' , starts at quadratic order. We have also noted above the connection of our finding from the series analysis that γ'_ℓ for the honeycomb lattice has twice the value of the corresponding γ' exponent for the singularity at $u = -1/3$ on the triangular lattice with the exact relation (2.11). Since each of the exponents on the left-hand side of eq. (6.3.1) has twice the value of the respective exponent for the corresponding singularity at $u = -1/3$ on the triangular lattice, and since this is a linear equation, the right-hand side is also twice the value of 2 which holds for the triangular lattice.

One may also consider the analogous equation for the approach to $z = -1$ from within the complex-temperature extension of the AFM phase. We have extracted the exact value $\alpha'_{\ell,AFM} = 2$ in eq. (3.2.1) and, as discussed above, given the loose-packed nature of the honeycomb lattice and the resultant relation (4.6), it follows that the staggered magnetisation diverges with the exponent $\beta_{\ell,st} = \beta_\ell = -1/4$ as one approaches the point $z = -1$ from within the complex-temperature AFM phase. Combining these exact results with the conclusion from our analysis of the low-temperature series for the staggered susceptibility that $\alpha'_{\ell,a} = 5/2$, we find

$$\alpha'_{\ell,AFM} + 2\beta_{\ell,st} + \gamma'_{\ell,a} = 4 \quad (6.3.2)$$

in complete analogy with eq. (6.3.1), as expected for a loose-packed lattice.

6.4 Critical Amplitude for $\chi^{(a)}$ at $z = -1$

In order to calculate the critical amplitude $A'_{\ell,a}$ in the staggered susceptibility as one approaches $z = y = -1$ from the complex AFM phase, we compute the series for $(\bar{\chi}_r^{(a)})^{1/\gamma'_{\ell,a}}$ using our inferred value $\gamma'_{\ell,a} = 5/2$. Since the exact function $(\bar{\chi}_r^{(a)})^{1/\gamma'_{\ell,a}}$ has a simple pole at $z = -1$, one performs the Padé analysis on the series itself instead of its logarithmic derivative. The residue at this pole is $-y_\ell(A'_{\ell,a,r})^{1/\gamma'_{\ell,a}}$, where $A'_{\ell,a,r}$ denotes the critical amplitude for $\bar{\chi}_r^{(a)}$. Extracting $A'_{\ell,a,r}$ and multiplying by the prefactor, we obtain $A'_{\ell,a} = 4y_\ell^3 A'_{\ell,a,r} = -4A_{\ell,a,r}$:

$$A'_{\ell,a} = -0.700 \pm 0.010 \quad (6.4.1)$$

An analysis of the series for $\bar{\chi}_r^{1/\gamma'_\ell}$ to extract the critical amplitude for the (uniform) susceptibility as one approaches $z = -1$ from within the complex FM phase did not yield precise

results, presumably because of the shortness of the series. However, having already inferred that $\bar{\chi}$ and $\bar{\chi}^{(a)}$ have the same power-law divergence at $z = y = -1$, as approached from the complex FM and AFM phases, respectively, we can use the relation (2.11) to compute A'_ℓ indirectly. For this purpose, we recall that on the triangular lattice, at the corresponding point $u = u_e = -1/3$, the (uniform) susceptibility $\bar{\chi}_t$ has the leading singularity [5, 10]

$$\bar{\chi}_t \sim A'_{e,t}(1 + 3u)^{-5/4} \quad (6.4.2)$$

Using this, together with the Taylor series expansion (3.2.3), we find the following relations among the critical amplitude $A'_{e,t}$ at $u = -1/3$ on the triangular lattice and A'_ℓ and $A'_{\ell,a}$ at $z = -1$ on the honeycomb lattice:

$$2 \cdot 3^{5/4} A'_{e,t} = A'_\ell + A'_{\ell,a} \quad (6.4.3)$$

We next use our previous determination of $A'_{e,t}$ [10]

$$A'_{e,t} = -0.05766 \pm 0.00015 \quad (6.4.4)$$

which agrees with, and has somewhat smaller uncertainty than, an earlier determination of this quantity by Guttman [5]. Substituting (6.4.1) and (6.4.4) into (2.11), we obtain the critical amplitude for the uniform susceptibility,

$$A'_\ell = 0.245 \pm 0.010 \quad (6.4.5)$$

7 Other Singularities

We also used the low-temperature series for $\bar{\chi}$ and $\bar{\chi}^{(a)}$ to investigate the singular behaviour of these functions as one approaches the points $z = z_{s\pm} = \pm i$ from within the complex-temperature FM and AFM phases, respectively. However, we were not able to obtain conclusive results. This is similar to our previous experience investigating the behaviour of $\bar{\chi}$ on the triangular lattice in the vicinity of the singular point $u = -1$ as approached from within the complex FM phase. These points, i.e., $z = \pm i$ on the honeycomb lattice and $u = -1$ or equivalently $z = \pm i$ on the triangular lattice, share in common the property that they are intersection points where two arcs of the complex-temperature phase boundary curves cross.

Concerning singularities of $\bar{\chi}$ and $\bar{\chi}^{(a)}$ elsewhere on the boundaries of the complex-temperature FM and AFM phases, respectively, it is quite possible that these functions may exhibit discontinuities, as we found for C and M . As is well-known from work on first-order phase transitions, the analysis of the low-temperature series by itself, and similarly, the high-temperature series by itself, does not, in general, provide a sensitive probe for such

discontinuities. Of course if one had sufficiently long series, the comparison of the limits as one approached a phase boundary from, say, the FM and the PM phases using the respective low- and high-temperature series, could be of value in this regard.

8 Behaviour of $\bar{\chi}$ in the Symmetric Phase

The theorem proved in Ref. [7] and discussed further in Ref. [9] implies that, for the Ising model on the square lattice, $\bar{\chi}$ has at most finite non-analyticities as one approaches the boundary of the complex-temperature extension of the PM phase, aside from the physical critical point at $v = v_c$. We would expect a similar theorem to hold for the honeycomb lattice, although to show this with complete rigour, it would be desirable to perform an analysis of the asymptotic behaviour of the general connected 2-spin correlation function $\langle \sigma_{0,0} \sigma_{m,n} \rangle$ as $r = (m^2 + n^2)^{1/2} \rightarrow \infty$ for this lattice, which has not, to our knowledge, been done. Assuming that such a theorem does hold, it would follow, in particular, that, $\bar{\chi}(v)$ and $\bar{\chi}^{(a)}(v) = \bar{\chi}(-v)$ would have finite non-analyticities as one approaches the points $v = \pm i$ from within the PM phase. We have analysed the high-temperature series expansion for $\bar{\chi}(v)$ to investigate the singularities at $v = \pm i$. This series is of the form

$$\bar{\chi} = 1 + \sum_{n=1}^{\infty} a_n v^n \quad (8.1)$$

It has a finite radius of convergence and, by analytic continuation from the physical high-temperature interval $0 \leq v < v_c$, applies throughout the complex extension of the PM phase. The high-temperature series expansion (8.1) is known to $O(v^{32})$ [23, 17]. Since we anticipated a finite singularity, we analysed this series using differential approximants, which are capable of representing this type of singularity in the presence of an analytic background term. However, as we recall from Fig. 1(c), there are two semi-infinite line segments which protrude into the complex-temperature PM phase, with endpoints at $v = \pm v_e = \pm i/\sqrt{3}$. We found that the series are not sensitive to the singularities at $v = \pm i$, presumably because of the effect of the intervening singular line segments and their endpoints at $v = \pm i/\sqrt{3}$. We have also tried to study the singularities in $\bar{\chi}$ at these endpoints. Again, our study did not yield an accurate value for the exponent γ_e , presumably due to the insufficient length of the series. However, the (scattered) values of γ_e were consistent with the expectation that $\gamma_e < 0$.

9 Conclusions

In this paper we have investigated complex-temperature singularities in the Ising model on the honeycomb lattice. As part of this, we have discussed the complex-temperature phases and their boundaries. From exact results, we have determined these singularities completely for the specific heat and the uniform and staggered magnetisation. From an analysis of low-temperature series expansions, we have found evidence that χ and $\chi^{(a)}$ both have divergent singularities at $z = -1 \equiv z_\ell$ (where $z = e^{-2K}$), with exponents $\gamma'_\ell = \gamma'_{\ell,a} = 5/2$. The critical amplitudes at this singularity were calculated. We have found that the linear combination of exponents $\alpha' + 2\beta + \gamma'$ is equal to 4 rather than 2 at $z = -1$. The connection of these results to corresponding complex-temperature singularities on the triangular lattice was discussed. Finally, some results on complex-temperature singularities reached from within the symmetric phase were given.

One of us (RS) would like to thank Profs. David Gaunt and Tony Guttmann for information about the current status of the series expansions for the honeycomb lattice. This research was supported in part by the NSF grant PHY-93-09888.

References

- [1] Onsager, L. 1944 *Phys. Rev.* **65** 117.
- [2] Yang, C. N. 1952 *Phys. Rev.* **85** 808.
- [3] Thompson, C. J., Guttmann, A. J., Ninham, B. W. 1969 *J. Phys. C* **2** 1889; Guttmann, A. J. 1969 *ibid*, 1900.
- [4] Domb, C. and Guttmann, A. J. 1970 *J. Phys. C* **3** 1652.
- [5] Guttmann, A. J. 1975 *J. Phys. A: Math. Gen.* **8** 1236.
- [6] Fisher, M. E. 1965 *Lectures in Theoretical Physics* (Univ. of Colorado Press, Boulder), vol. 12C, p. 1.
- [7] Marchesini, G. and Shrock, R. 1989 *Nucl. Phys. B* **318** 541.
- [8] Enting, I. G., Guttmann, A. J., and Jensen, I. 1994 “Low-Temperature Series Expansions for the Spin-1 Ising Model” (April, 1994), *J. Phys. A: Math. Gen.*, in press.

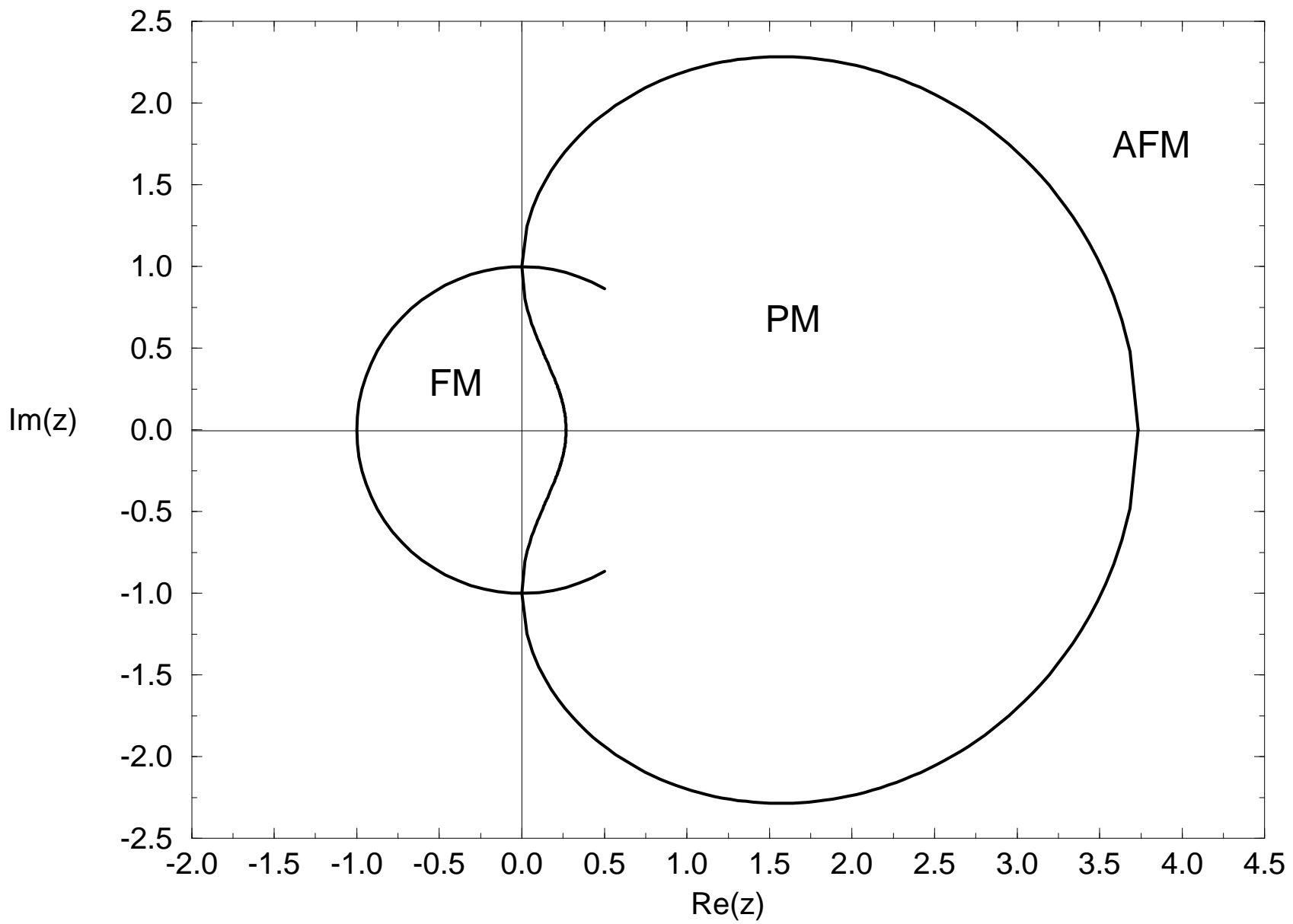
- [9] Matveev, V. and Shrock, R., “Complex-Temperature Singularities of the Susceptibility in the $d = 2$ Ising Model. I. Square Lattice” ITP-SB-94-37 (Aug. 1994) (hep-lat/9408020), *J. Phys. A: Math. Gen.*, in press.
- [10] Matveev, V. and Shrock, R., “Complex-Temperature Singularities in the $d = 2$ Ising Model. II. Triangular Lattice” ITP-SB-94-53 (Nov. 1994) (hep-lat/9411023), submitted to *J. Phys. A: Math. Gen.*.
- [11] Itzykson, C., Pearson, R., and Zuber, J.B. 1983 *Nucl. Phys. B* **220** 415.
- [12] Houtappel, R. M. F. 1950 *Physica* **16** 425; Syozi, I. 1950 *Prog. Theor. Phys.* **5** 341; Temperley, H. N. V. 1950 *Proc. Roy. Soc.* **A202** 202.
- [13] Naya, S. 1954 *Prog. Theor. Phys.* **11** 53.
- [14] Lefschetz, S. 1953 *Algebraic Geometry* (Princeton Univ. Press, Princeton); Hartshorne, R. 1977 *Algebraic Geometry* (Springer, New York).
- [15] Sykes, M. F., Gaunt, D. S., Martin, J. L, Mattingly, S. R., and Essam, J. W. 1973 *J. Math. Phys.* **14** 1071.
- [16] Sykes, M. F., Watts, M. G., and Gaunt, D. S. 1975 *J. Phys. A: Math. Gen.* **8** 1448.
- [17] Gaunt, D. S. 1994, private communication.
- [18] Guttmann, A. J. 1994, private communication.
- [19] Guttmann, A. J. 1989 in *Phase Transitions and Critical Phenomena*, Domb, C. and Lebowitz, J., eds. (Academic Press, New York) vol. 13.
- [20] Fisher, M. E. 1959 *Phys. Rev.* **113** 969.
- [21] Domb, C. 1960 *Adv. in Phys.* **9** 149.
- [22] Potts, R. B. 1952 *Phys. Rev.* **88** 352.
- [23] Sykes, M. F., Gaunt, D. S., Roberts, P. D., and Wyles, J. A. 1972 *J. Phys. A: Math. Gen.* **5** 624.

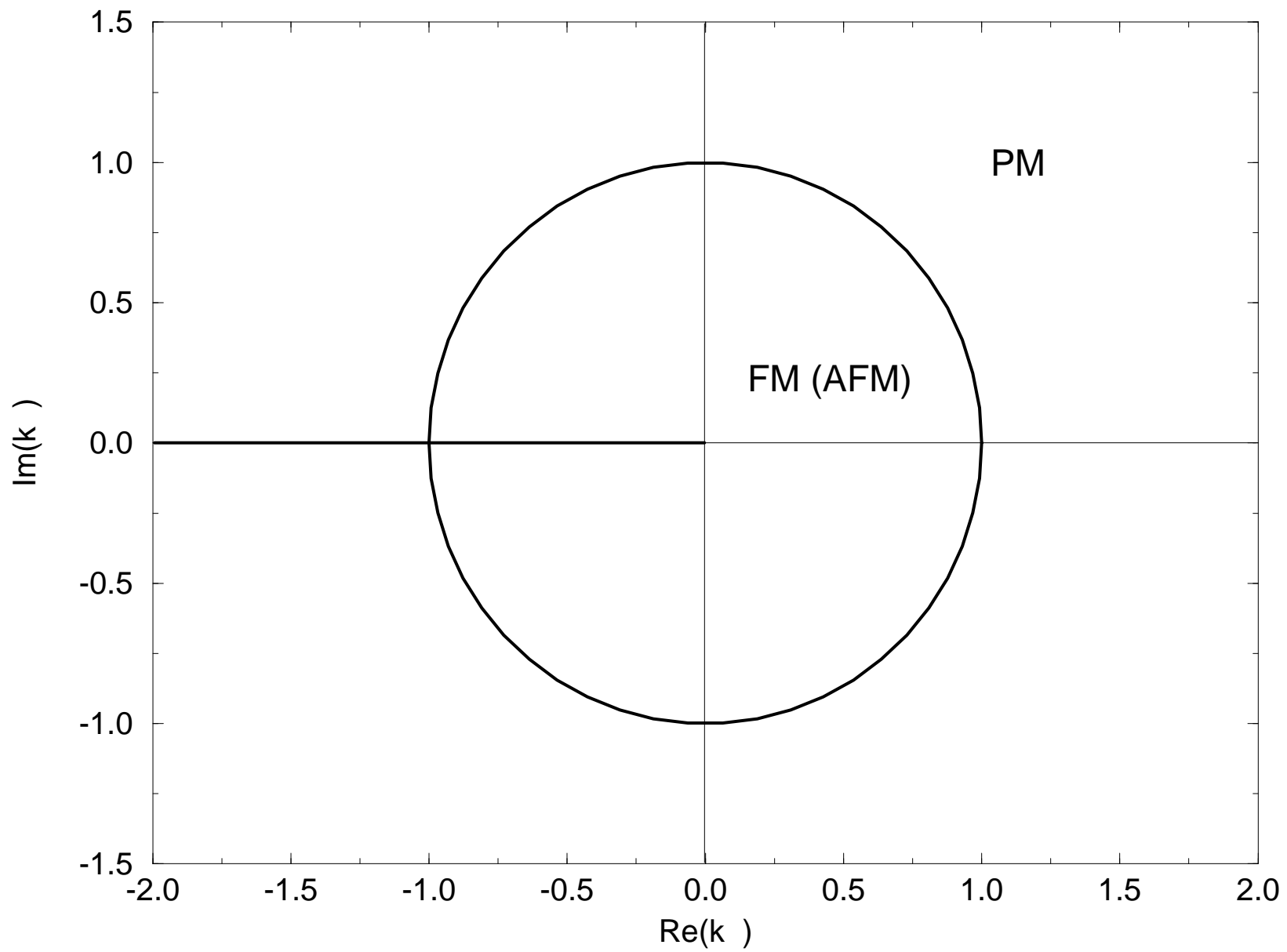
Figure Caption

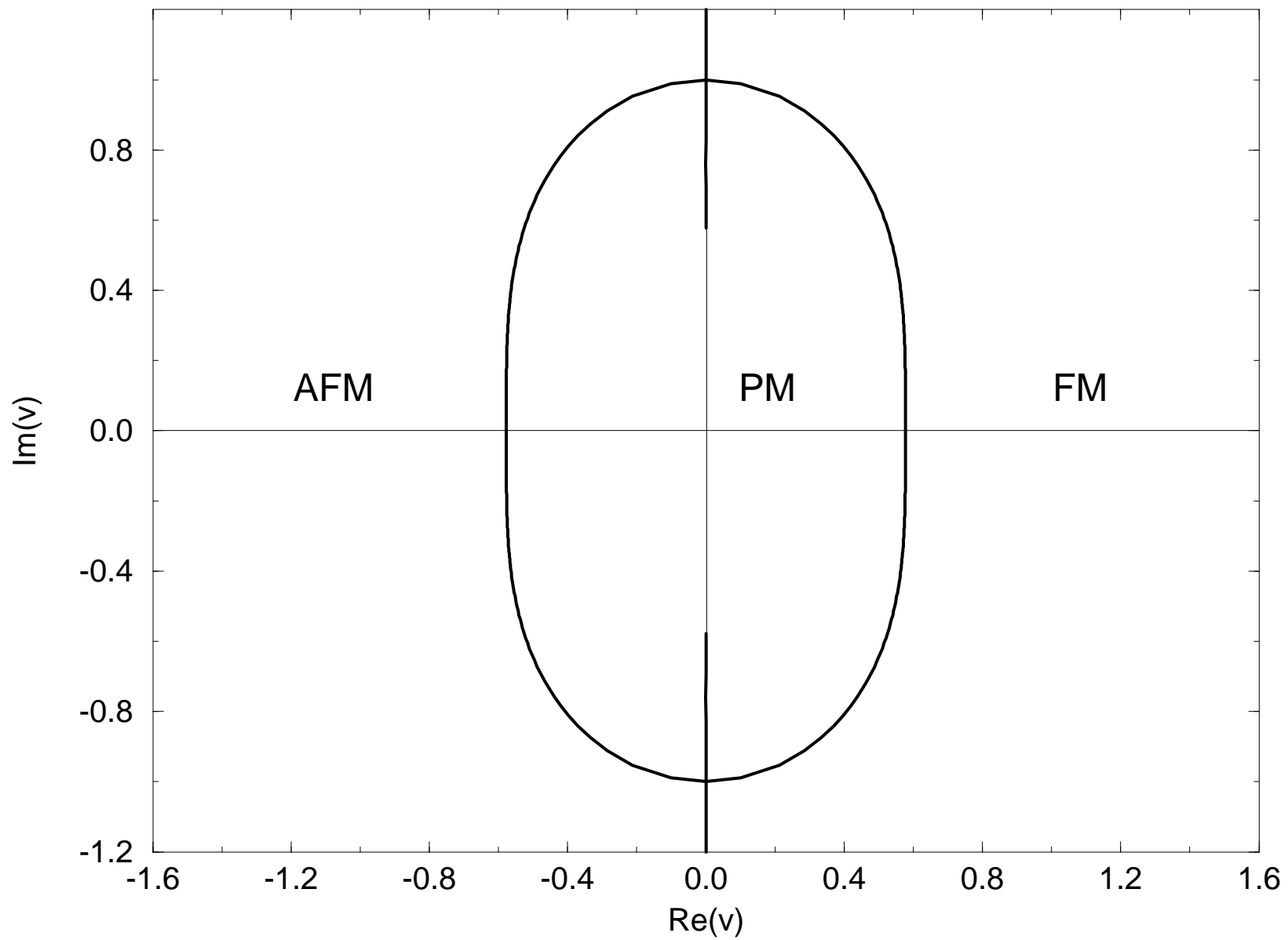
Fig. 1. Complex-temperature phases and associated boundaries in the variables (a) z , (b) $k_<$, and (c) v . FM, AFM, and PM denote ferromagnetic, antiferromagnetic, and paramagnetic, Z_2 -symmetric phases. In Fig. 1(b), the semi-infinite line segment extends along the negative real axis from $k_< = 0$ to $k_< = -\infty$. In Fig. 1(c), the semi-infinite line segments extend along the imaginary axis from $v = \pm i/\sqrt{3}$ to $\pm i\infty$, respectively.

This figure "fig1-1.png" is available in "png" format from:

<http://arxiv.org/ps/hep-lat/9412076v1>







This figure "fig1-2.png" is available in "png" format from:

<http://arxiv.org/ps/hep-lat/9412076v1>

This figure "fig1-3.png" is available in "png" format from:

<http://arxiv.org/ps/hep-lat/9412076v1>